Journal of Petroleum Science and Engineering 143 (2016) 8–13

Contents lists available at ScienceDirect

Journal of Petroleum Science and Engineering

journal homepage: www.elsevier.com/locate/petrol

The origin and evolution of thermogenic gases in organic-rich marine shales

Yongqiang Xiong *, Li Zhang, Yuan Chen, Xiaotao Wang, Yun Li, Mingming Wei, Wenmin Jiang, Rui Lei

State Key Laboratory of Organic Geochemistry (SKLOG), Guangzhou Institute of Geochemistry, Chinese Academy of Sciences, Guangzhou 510640, PR China

ARTICLE INFO

Article history:
Received 15 November 2015
Received in revised form
6 February 2016
Accepted 15 February 2016
Available online 16 February 2016

Keywords:
Shale gas
Marine shale
Kerogen
Bitumen
$\delta^{13}C$
Simulation experiment

ABSTRACT

In order to better understand the generation and primary source of mature thermogenic gas in shale, and to evaluate the residual gas generation potential of the shale at different maturity levels, we performed pyrolysis experiments on an organic-rich marine shale and its kerogens prepared by artificial maturation. The results indicate that the thermal maturation of organic matter in the shale can be divided into four stages: oil generation ($<$ 0.6–1.0% EasyRo), condensate generation (1.0–1.5% EasyRo), wet gas generation (1.5–2.2% EasyRo), and dry gas generation (2.2–4.5% EasyRo). Thermogenic methane is produced mainly during wet gas and dry gas generation, while most of the C_{2+} hydrocarbon gases are produced during condensate and wet gas generation. The kerogen at a thermal maturity of $>$ 3.0% EasyRo still has methane generation potential. Whether or not gas generation potential of a highly mature kerogen has a commercial significance depends on its organic matter richness, thermal maturity internal and some other geological factors, such as caprock sealing property, reservoir physical property, and tectonic movement. In addition to the gas produced from kerogen cracking, gas is also generated from the secondary cracking of residual bitumen as maturation progresses. Early hydrocarbon expulsion during oil generation likely has a considerable effect on the amount and $\delta^{13}C$ values of the late-generated shale gas. The lower the oil expulsion efficiency of a shale, i.e., the more retained bitumen, then the higher the productivity of post-mature shale gas and comparative enrichment of the latter in ^{12}C.

1. Introduction

Hydrocarbon generation potential is commonly assessed by the abundance, type, and thermal maturity of organic matter in source rocks. Productive shale gas formations in North America generally have $>$ 2.0% TOC, type II kerogen, and $>$ 1.3% (vitrinite reflectance equivalent) thermal maturity (Zumberge et al., 2012). However, the geological settings of organic-rich, marine shale formations in China are distinct from those in North America. In China, shale gas formations are characterized by old strata, deep burial, high thermal maturity, and multi-stage tectonism (Dai et al., 2014; Zou et al., 2015). Therefore, more targeted criteria are needed to evaluate shale gas generation potential in China. Investigations into the origin and formation mechanism of highly mature and over-mature shale gas, the upper limit of maturation for gas generation from marine kerogens, and the effect of intense tectonism on the deformation and alteration of shale gas reservoirs are more critical for Chinese shale gas exploration.

Shale gas is natural gas trapped within shale, which has biogenic and thermogenic origins (Martini et al., 1998; Jarvie et al., 2007). The sources of thermogenic gas in shale include kerogen (insoluble organic matter), bitumen (soluble organic matter), and often pyrobitumen (a residue of bitumen cracking) (Jarvie et al., 2007) (Fig. 1). Different gas generation stage and gas generation potential result in the changes of their relative contributions to shale gas with thermal maturation. For example, during early maturation, little gas is produced together with the formation of bitumen, and the gas is derived mainly from the primary cracking of kerogen. With increasing maturity, bitumen (as the intermediate of kerogen cracking) becomes an important source of gas. During late maturation, a large amount of gas is produced from the cracking of both kerogen and bitumen. Because kerogen does not migrate out of the source rock, its contribution to gas generation is relatively stable and simple to evaluate. On the other hand, the gas contribution of bitumen depends on the hydrocarbon expulsion efficiency of shale (Fig. 1). The cracking of oil, or expelled bitumen, is considered the major source of conventional gas generated from hydrogen-rich marine source rocks (Welte et al., 1988; Rooney et al., 1995). Conventional and unconventional gas fields commonly occur together within a hydrocarbon basin (Zou et al.,

* Corresponding author.
E-mail address: xiongyq@gig.ac.cn (Y. Xiong).

http://dx.doi.org/10.1016/j.petrol.2016.02.008
0920-4105/

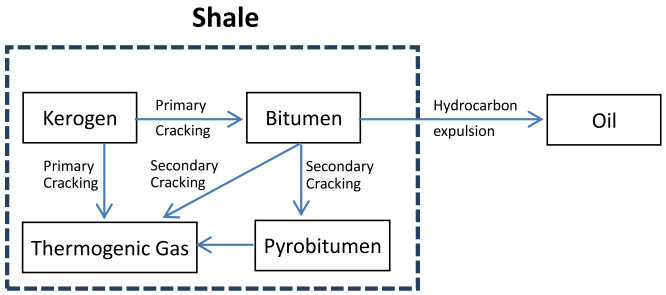

Fig. 1. Process of the indigenous generation of thermogenic gas in shale (modified from Jarvie et al., 2007).

2015), where the cracking of expelled oil produces conventional gas, and the cracking of retained oil (i.e., bitumen) and kerogen generates unconventional gas. As more oil is expelled, less bitumen is retained in the shale to generate unconventional gas. Therefore, high hydrocarbon expulsion efficiency at peak oil generation is favorable for the generation of conventional gas, but unfavorable for the generation of unconventional gas.

At present, no method can effectively determine the hydrocarbon expulsion efficiency of source rocks. The simulation of hydrocarbon expulsion under actual geological conditions is also difficult. Gai et al. (2015) used an artificial mix of kerogen and its extracts to design a suite of samples with variable oil expulsion efficiencies, and performed pyrolysis experiments to analyze the effect of oil expulsion efficiency on shale gas generation in a closed system. During shale maturation, however, bitumen is an intermediate product with an evolving concentration, composition, and gas generation potential. Thus, hydrocarbon expulsion is a dynamic process, and its contribution to gas generation depends on thermal maturity.

The purpose of this study was to improve our understanding of the generation mechanisms of, and precursors to, shale gas in mature organic-rich marine shale, and to evaluate the effect of hydrocarbon expulsion on shale gas potential. A series of laboratory simulations was performed on a marine shale and its kerogens using artificial maturation. The pyrolysis of the source rock and its original kerogen was used to simulate the generation of shale gas in a closed system. The combination of artificial maturation and closed gold tube pyrolysis was used to obtain the residual gas generation from kerogens at various levels of thermal maturity.

2. Experimental methods

2.1. Samples

The marine shale sample used in this study was collected from the upper Proterozoic Xiamaling Formation in the Xiahuayuan region of Zhangjiakou City, Hebei Province, China. The geochemical characterization of the Xiamaling Formation in this area had been described by Zhang et al. (2007). This shale contains type II kerogen with a low T_{max} value of 434 °C, a vitrinite-like maceral reflectance (Ro) value of 0.57%, and a relatively high TOC content of 6.78 wt%. Prior to analysis, the surface of the sample was cleaned with dichloromethane, and the shale was ground to 100 mesh. We performed a sealed gold tube pyrolysis experiment on the shale to simulate the generation of shale gas and to assess its maximum gas yield.

The source rock sample was demineralized in a water bath (80 °C) with hydrochloric and hydrofluoric acids to isolate kerogen that was then ground to 100 mesh. The kerogen concentrate was Soxhlet-extracted for 72 h with dichloromethane:methanol (93:7 v/v) to remove soluble organic matter, and was then dried at 50 °C for 12 h. This kerogen represents the original kerogen before oil generation (K_1). The other three kerogen samples (K_2, K_3, and K_4) were prepared by artificial maturation of the original kerogen (K_1) over the full thermal range of oil generation. The artificial maturation process was performed in a vacuum glass tube. Heating temperature and times were based on the EasyRo method of Sweeney and Burnham (1990) (Table 1). The kerogen was Soxlet-extracted with dichloromethane for 72 h to remove newly produced soluble organic matter, and was used to simulate the formation of gas from kerogen cracking at various stages of maturation.

Table 1
Conditions for the preparation of kerogen samples used in the simulation experiments.

Kerogen	Maturity (% EasyRo)	Heating temperature (°C)	Heating time (h)	Residual rate (%)[a]	TOC (wt%)
K_1	0.57	–	–	100	68.12
K_2	0.80	320	57	85.7	73.77
K_3	1.0	345	65	82.4	69.92
K_4	1.3	365	95	77.2	72.56

[a] The ratio is calculated by kerogen mass before and after heating

2.2. Pyrolysis experiments

Pyrolysis experiments on the marine shale (whole rock) and four extracted kerogens representing four stages of maturation (0.57% VRo, 0.80%, 1.0%, and 1.3% EasyRo) were carried out in sealed gold tubes following Xiong et al. (2004). Aliquots of 10–50 mg kerogen or 50–100 mg whole-rock shale were loaded into gold tubes (40 mm length, 4.2 mm inside diameter, and 0.25 mm wall thickness) before being purged with argon for 5 min and sealed under an argon atmosphere. The sealed gold tubes were placed in stainless steel autoclaves that were heated in an oven at two constant heating rates of 20 °C/h and 2 °C/h, under constant pressure of 50 MPa. Sampling was conducted at ca. 24 °C intervals between 336 °C and 600 °C (12 total samples for each heating rate). After heating, the autoclaves were removed from the oven and cooled to room temperature.

2.3. Determination of pyrolytic products

The pyrolysates were analyzed to determine the chemical and carbon isotopic compositions of gaseous hydrocarbons using gas chromatography (GC) and gas chromatography–isotope ratio mass spectrometry (GC–IRMS). The cleaned gold tube for each temperature point was placed in a vacuum glass system connected to a GC inlet. After piercing the gold tube with a steel needle, the gaseous components were released and introduced into the GC system, where they were quantified using an Agilent Technologies 7890-0322 GC. The system had high sensitivity (as good as for the analysis of 0.01 mL volume of gas), good accuracy (with the relative errors being less than 0.5%). The analysis of all gaseous hydrocarbons (C_1–C_5) and other gas components (such as N_2, H_2 and CO_2) could be carried out with a single injection. The carbon isotopic compositions of gaseous hydrocarbons were determined on a GV Instruments Isoprime stable isotope mass spectrometer. Reported isotopic data represented the arithmetic means of at least two duplicate analyzes, and the repeatability was less than 0.3‰. All carbon isotopic values were reported in per mil (‰) relative to the VPDB standard.

The gold tube for the analysis of C_6–C_{12} hydrocarbons was cooled for about 30 min using liquid nitrogen, and then rapidly cut in half and placed in a 4 mL vial filled with methanol. The C_6–C_{12}

hydrocarbon compositions were then analyzed using headspace single-drop microextraction coupled with GC flame ionization detection (Fang et al., 2011). Briefly, fifty microliters of the sample was spiked into a 10 mL glass vial with 5 mL of water, and a magnetic stir bar, and an aluminum cap seal containing a PTFE-faced silicone septum. The vial was then placed on a magnetic stirrer (Jiangsu Guohua, China). A 10 μL microsyringe (SGE Analytical Science, Australia) was used as both the extraction and injection syringe. After a certain volume of extraction solvent containing n-$C_8{}^2H_{18}$ as the internal standard was drawn into the microsyringe, the syringe needle was inserted through the rubber septum of the sample vial until its tip was about 0.5 cm above the surface of sample solution. The micro syringe was fixed above the extraction vial by a metal clamp during the extraction. The syringe plunger was then carefully and slowly depressed until the micro drop of extraction solvent was suspended at the needle tip. After the extraction, the micro drop was retracted back into the needle carefully and slowly, and directly injected into the gas chromatography system for analysis.

3. Results and discussion

3.1. Generation of gaseous hydrocarbons during maturation

Fig. 2 shows the cumulative yields of methane, C_2–C_5 gaseous hydrocarbons (GHs), and C_6–C_{12} light hydrocarbons (LHs) during the artificial maturation of the whole-rock shale sample and its kerogen. The whole-rock and kerogen pyrolyses display a very similar evolution in terms of the yields of methane and C_2–C_5 GHs, but have distinct yield curves for the C_6–C_{12} LHs. On the basis of the partitioning of the oil cracking stage in the same pyrolysis system (Fang et al., 2012), we identify four main stages in the thermal maturation process of organic matter in shale rock or kerogen: oil generation (Stage I), condensate generation (Stage II), wet gas generation (Stage III), and dry gas generation (Stage IV). The onset of oil cracking occurred at ~1.0% EasyRo (Fang et al., 2012); consequently, the stage of maturation prior to oil cracking in this study is considered Stage I, corresponding to $<$0.6–1.0% EasyRo. Stage II corresponds to 1.0–1.5% EasyRo, which was characterized by the rapid generation of C_6-C_{12} LHs and a maximum yield at 1.5% EasyRo. Stage III corresponds to 1.5–2.2% EasyRo, during which the yield of C_6–C_{12} LHs rapidly decreased, and that of C_2–C_5 GHs gradually increased to a maximum at 2.2% EasyRo. At EasyRo $>$2.2%, the decomposition rate of C_2–C_5 GHs exceeded that of generation, indicating the onset of Stage IV, corresponding to 2.2–4.5% EasyRo.

During the whole-rock pyrolysis (Fig. 2a), the total yield of methane was ~282 mg/gTOC, only 4.3% (12 mg/gTOC) and 8.4% (24 mg/gTOC) of which was produced during stages I and II, respectively. The yields during Stages III and IV were 20.5% (58 mg/gTOC) and 66.8% (188 mg/gTOC), respectively, indicating that methane was mostly produced during wet gas and dry gas generation, accounting for 87.3% of the total methane yield. The whole-rock C_2–C_5 GHs were produced mainly between 0.7% and 2.2% EasyRo, with the maximum yield reaching ~167 mg/gTOC at 2.2% EasyRo, followed by decomposition (Fig. 2b). The relative yield of C_2–C_5 GHs was 13.5% (Stage I), 39.7% (Stage II), and 46.8% (Stage III). A slight difference in the yield of C_2–C_5 GHs during kerogen and whole-rock pyrolysis occurs at $>$1.7% EasyRo, with a lower maximum yield of C_2–C_5 GHs during kerogen pyrolysis than during whole-rock pyrolysis. Fig. 2c indicates that the C_6–C_{12} LHs are formed mainly during Stages I and II, and that the total yield for kerogen is considerably more than that for whole rock. The marked differences may be caused by the catalytic effect of mineral matrix (Tannenbaum and Kaplan, 1985).

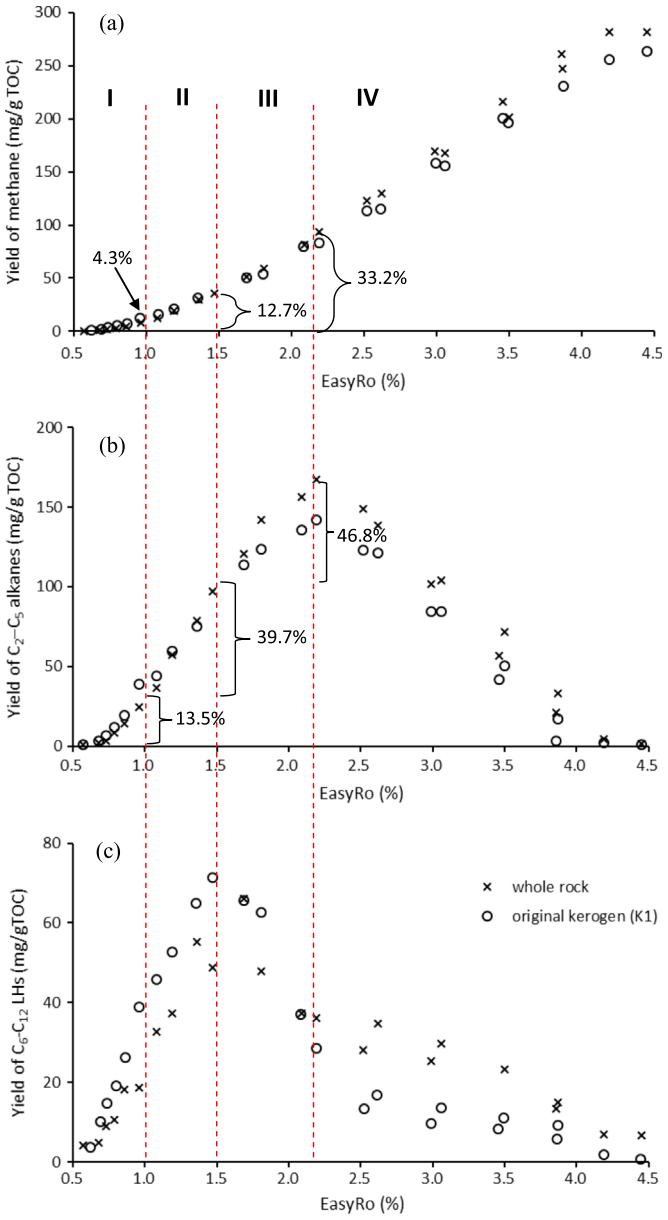

Fig. 2. Yield curves of (a) methane, (b) C_2–C_5 gaseous hydrocarbons, and (c) C_6–C_{12} light hydrocarbons generated from the artificial maturation of shale (whole rock) and its original kerogen (K_1). I – oil-generation stage, II – condensate-generation stage, III – wet-gas-generation stage, IV – dry-gas-generation stage.

3.2. Origin of gaseous hydrocarbons

To quantify the contributions of kerogen and bitumen to gaseous hydrocarbon generation in shales, and also to characterize the gaseous hydrocarbons generated at various stages of maturation, we analyzed four solvent-extracted kerogens (K_1, K_2, K_3, and K_4) to determine the residual gas generation potential of the kerogens at variable maturity (0.57% VRo, 0.80%, 1.0%, and 1.3% EasyRo). Fig. 3 shows the yield curves of methane, C_2–C_5 GHs, and C_6–C_{12} LHs for the four solvent-extracted kerogens.

With a thermal maturity of $<$1.3% EasyRo, little gas is produced from the secondary cracking of oil, based on extrapolation from the kinetic data of Waples (2000) (Hill et al., 2007). Thus, the gaseous hydrocarbons in the pyrolysate of original kerogen (K_1) at $<$1.3% EasyRo were derived mainly from the primary cracking of kerogen that accompanied oil formation. The yield of kerogen-cracked methane in this stage was relatively low (Fig. 3a), and

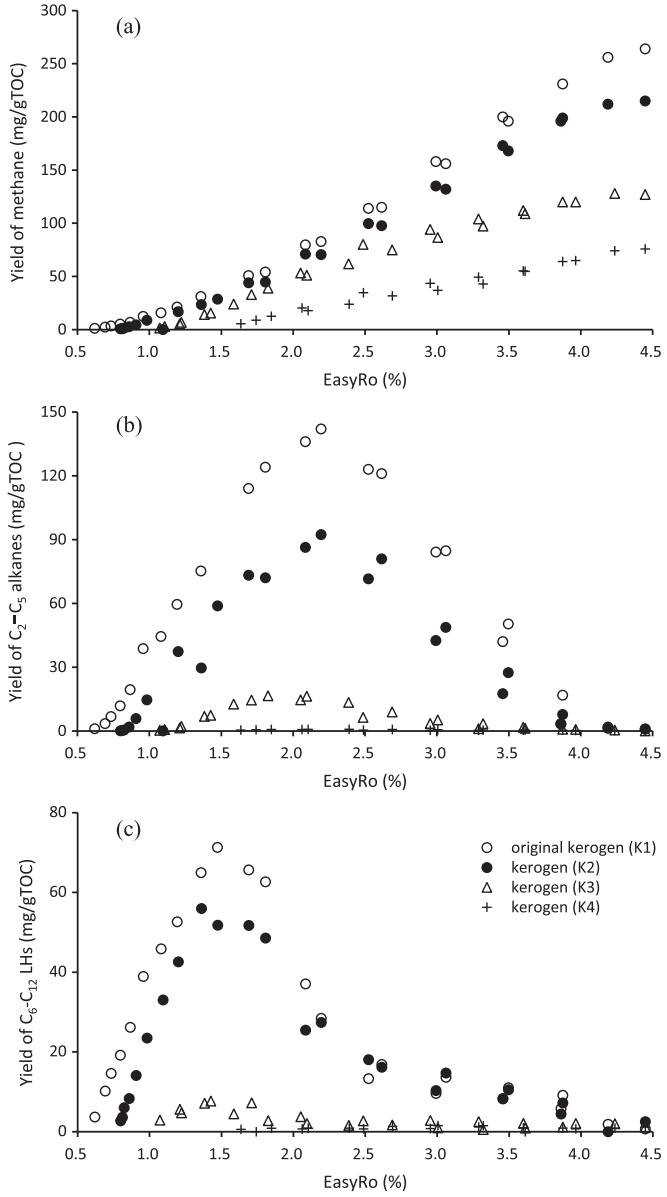

Fig. 3. Yield curves of (a) methane, (b) C_2–C_5 gaseous hydrocarbons, and (c) C_6–C_{12} light hydrocarbons generated from the four solvent-extracted kerogens representing different maturity levels (K_1 – original kerogen, 0.57% VRo; K_2 – 0.80% EasyRo, K_3 – 1.0% EasyRo, and K_4 – 1.3% EasyRo).

increased with maturation to ~24 mg/gTOC at 1.3% EasyRo, accounting for < 10% of the total methane yield. On the other hand, nearly half of the C_2–C_5 GHs and > 80% of the C_6–C_{12} LHs were generated at 0.6–1.3% EasyRo, mainly from the primary cracking of kerogen.

Few C_6–C_{12} LHs or C_2–C_5 GHs were produced from the K_4 kerogen (Fig. 3b and c), indicating that the extracted kerogen with a thermal maturity of > 1.3% EasyRo had no generation potential for C_{2+} hydrocarbons. Because the early generated hydrocarbons were removed during sample preparation of the K_4 kerogen, leaving almost no C_{2+} hydrocarbon-generating potential, the methane generated during the pyrolysis of K_4 kerogen (Fig. 3a) was produced mainly from the cracking of highly mature and overmature kerogen, and it accounted for ~29% (75.8 mg/gTOC) of the total methane yield. Therefore, we were able to construct the yield curve for kerogen-cracked methane (Fig. 4) by combining the methane yield curve of the K_4 kerogen with that of the original K_1 kerogen at < 1.3% EasyRo (Fig. 3). The weight of K_4 kerogen

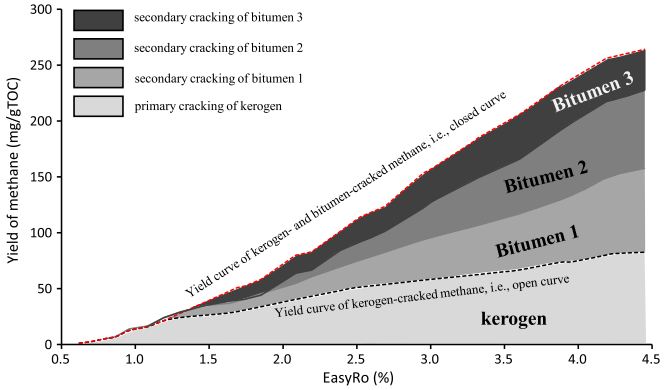

Fig. 4. Possible origins of methane during the maturation of original kerogen (K_1). Bitumen 1, 2, and 3 represent extractable organic matter generated during the maturation stages 0.57–0.8%, 0.8–1.0%, and 1.0–1.3% EasyRo, respectively.

obtained after artificial maturation was 77.2% of the K_1 kerogen weight (Table 1). As a result, the observed K_4 methane yield used in Fig. 4 was the corrected one relative to original kerogen, i.e., the measured K_4 yield (Fig. 3) was multiplied by 77.2%. Other K_2 and K_3 yields also were corrected with their residual rate data (Table 1) and used to construct the yield curve of bitumen-cracked methane. Because kerogen does not migrate out of its source rock, the yield curve of kerogen-cracked methane was not affected by hydrocarbon expulsion and it represents the minimum gas generation potential of the source shale under completely open conditions (i.e., no contribution from bitumen-cracked gas). Therefore, the yield of kerogen-cracked methane in the subject shale can be estimated based on the thermal maturity. Other shales will differ in lithology, kerogen composition and TOC.

The yield curve of original kerogen (K_1) reflects the total amount of gases generated during pyrolysis in a closed system, including the primary gases generated from kerogen cracking and the secondary gases generated from the cracking of residual oil and its intermediate products, hereafter termed 'bitumen'. Therefore, K_1 yield is the maximum gas generation potential of this shale during maturation under completely closed conditions. When thermal maturity is > 1.3% EasyRo, the cracking of kerogen-produced bitumen becomes an important additional source of gas in a closed system. The gas generation capacity of bitumen at various stages of maturity can be calculated by processes of subtraction. Let $Y_{res,\ i}$, the residual gas yield of the kerogen, equal the measured methane yield of extracted kerogens at various levels of maturity, i, given by K_2, K_3, and K_4 (Fig. 3). Let $Y_{k,\ 0}$ equal the gas yield of original kerogen (K_1), including kerogen-cracked methane and bitumen-cracked methane. The bitumen-cracked methane yields of the kerogen, $Y_{b,\ i}$, are given by Eq. (1).

$$Y_{b,i} = Y_{k,0} - Y_{\mathrm{res},i} \quad (1)$$

The calculated yield curves for bitumen-cracked methane are presented in Fig. 4, in which bitumen 1, 2, and 3 represent extractable organic matter generated during the maturation stages 0.57–0.8%, 0.8–1.0%, and 1.0–1.3% EasyRo, respectively.

Due to hydrocarbon expulsion under actual geological conditions, the gas yield for a source rock should fall between the 'open curve' (kerogen-cracked methane) and the 'closed curve' (Fig. 4). The higher the hydrocarbon expulsion efficiency during the early stages of shale maturation the lower the contribution from bitumen cracking. Thus, the gas yield will be more similar to the 'open curve' in Fig. 4. In addition, the estimated result (Fig. 4) shows that the bitumens produced between 0.57% and 1.0% EasyRo (i.e., bitumen 1 and bitumen 2) are major precursors of secondary cracking gas. Therefore, hydrocarbon expulsion occurring within

this maturity stage has a considerable effect on the amount of the late-generated shale gas.

Chen et al. (2007) suggested that the upper limit of maturity (i.e., the "deadline") for natural gas generation in marine type I and II kerogens is equal to 3.0% of the vitrinite reflectance (Ro). Our results indicate that the kerogen occurs at 3.0% EasyRo still has methane generation potential (Fig. 4). Whether or not gas generation potential of a highly mature kerogen has a commercial significance depends on its organic matter richness, thermal maturity internal and some other geological factors, such as caprock sealing property, reservoir physical property and tectonic movement.

3.3. *Possible influence of hydrocarbon expulsion on the $\delta^{13}C$ values of gaseous hydrocarbons*

Stable carbon isotopic compositions of gaseous hydrocarbons have been widely used to identify the origin of natural gases, and to assess their thermal maturity (Stahl, 1974; Schoell, 1983; James, 1990; Rooney et al., 1995). Our experimental results indicate that in addition to source and thermal maturity, hydrocarbon expulsion is also a possible factor influencing the carbon isotopic compositions of gaseous hydrocarbons.

The carbon isotope curve for hydrocarbon gases from the K_4 kerogen pyrolysis shows the variation in $\delta^{13}C$ values for kerogen-cracked gas at higher stages of maturity (> 1.3% EasyRo) (Fig. 5). The variation in $\delta^{13}C$ represents an extreme case of up to 100% hydrocarbon expulsion efficiency during the oil generation stage, although such a high efficiency may not occur under actual geologic conditions. We observed a trend of gradual $\delta^{13}C$ enrichment with thermal maturity for the late kerogen-cracked gas (> 1.3% EasyRo).

The gas produced from the K_1 kerogen pyrolysis experiment includes the total volume of gases that can be generated from the original kerogen. Therefore, the carbon isotope curves of K_1 kerogen pyrolysis, which can also be called as the 'closed curve', show variations in the $\delta^{13}C$ values of methane, ethane, and propane with thermal maturation in a completely closed system (Fig. 5). They are relatively depleted in ^{13}C, indicating that the bitumen-cracked gas has strongly negative $\delta^{13}C$ values compared with those of the kerogen-cracked gas. Compared with the gases generated during K_1 kerogen pyrolysis, less gas during the K_2 or K_3 kerogen pyrolysis experiments was generated from primary cracking (0.6–0.80% EasyRo or 0.6–1.0% EasyRo, respectively), or from the secondary cracking of bitumen formed during the two maturity stages. The carbon isotope curves of gaseous hydrocarbons fall between the 'late kerogen-cracked gas curve' and the 'closed curve' (Fig. 5), illustrating the role of degree of expulsion on gas $\delta^{13}C$ values as encountered in nature.

In addition, Fig. 5 shows that the isotope curves for the kerogens at various stages of maturity overlap in the oil generation stage, indicating that hydrocarbon expulsion has no obvious effect on the carbon isotope composition of hydrocarbon gases generated during this stage. Carbon isotope compositions diverge at ~1.2% EasyRo, at which point the increasing influence of bitumen-cracked gas during the gas generation stage leads to a substantial preferential losses of ^{12}C. The degree of carbon isotope fractionation peaks at 9‰ for methane and 12‰ for ethane. Low porosity, low permeability organic-rich shale is a good hydrocarbon adsorbent, leading to a relatively low hydrocarbon expulsion efficiency. Therefore, a shale with a lower hydrocarbon expulsion efficiency will produce more abundant gaseous hydrocarbons that are comparatively rich in ^{12}C at any given stage of maturation.

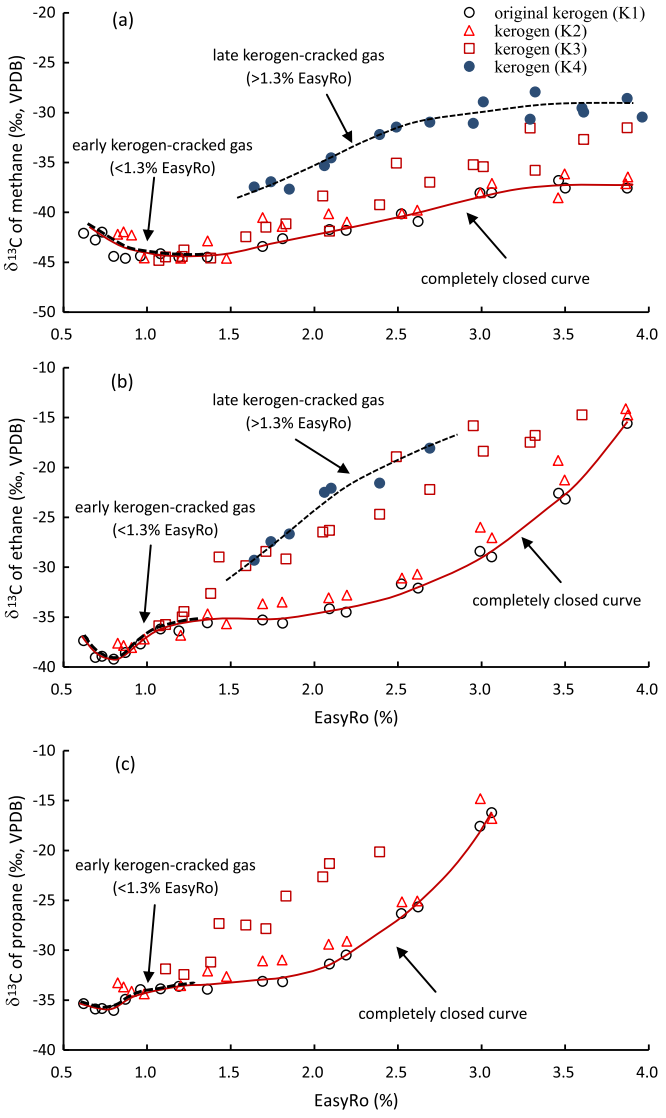

Fig. 5. Carbon isotope curves of (a) methane, (b) ethane and (c) propane generated from the four solvent-extracted kerogen (K_1, K_2, K_3, and K_4) representing different maturity levels.

4. Conclusions

The purpose of this study was to improve our understanding of the formation mechanism and main source of thermogenic gas in mature organic-rich marine shale through laboratory simulations on a marine shale and its kerogens using artificial maturation. The main conclusions are as follows:

(1) Thermogenic methane in shale gas is produced mainly during wet gas and dry gas generation, while C_{2+} hydrocarbon gases are generated during condensate and wet gas generation.
(2) The kerogen at a thermal maturity of > 3.0% EasyRo still has methane generation potential.
(3) In addition to the gas generated by kerogen cracking, more gases are derived from the secondary cracking of retained bitumen in highly mature and over-mature shale.
(4) Hydrocarbon expulsion during oil generation has a considerable effect on the amount and $\delta^{13}C$ values of late-generated shale gas.

Acknowledgments

This work was financially supported by the programs of the Chinese Academy of Sciences (Grant no. XDB10010500) and the Chinese Ministry of Land and Resources (Grant no. Zi[2014]03-030-003). We are grateful to Dr. K.F. Thompson and two anonymous reviewers for their useful comments and suggestions. This is contribution no. IS-2190 from GIGCAS.

Appendix A. Supplementary material

Supplementary data associated with this article can be found in the online version at http://dx.doi.org/10.1016/j.petrol.2016.02.008.

References

Chen, J.P., Zhao, W.Z., Xiao, Z.Y., Zhang, S.C., Deng, C.P., Sun, Y.G., Wang, Z.,M., 2007. A discussion on the upper limit of maturity for gas generation by marine kerogens and the utmost of gas generative potential: taking the study on the Tarim Basin as an example. Chin. Sci. Bull. 52 (Supp.1), S125–S132.

Dai, J.X., Zou, C.N., Liao, S.M., Dong, D.Z., Ni, Y.Y., Huang, J.L., Wu, W., Gong, D.Y., Huang, S.P., Hu, G.Y., 2014. Geochemistry of the extremely high thermal maturity Longmaxi shale gas, southern Sichuan Basin. Org. Geochem. 74, 3–12.

Fang, C.C., Xiong, Y.Q., Liang, Q.Y., Li, Y., Peng, P.A., 2011. Optimization of headspace single-drop microextration technique for extraction of light hydrocarbon (C_6-C_{12}) and its potential applications. Org. Geochem. 42, 316–322.

Fang, C.C., Xiong, Y.Q., Liang, Q.Y., Li, Y., 2012. Variation in abundance and distribution of diamondoids during oil cracking. Org. Geochem. 47, 1–8.

Gai, H.F., Xiao, X.M., Cheng, P., Tian, H., Fu, J.M., 2015. Gas generation of shale organic matter with different contents of residual oil based on a pyrolysis experiment. Org. Geochem. 78, 69–78.

Hill, R.J., Zhang, E.T., Katz, B.J., Tang, Y.C., 2007. Modeling of gas generation from the Barnett shale, Fort Worth Basin, Texas. Am. Assoc. Pet. Geol. Bull. 91, 501–521.

James, A., 1990. Correlation of reservoired gases using the carbon isotopic compositions of wet gas components. Am. Assoc. Pet. Geol. Bull. 74, 1441–1458.

Jarvie, D.M., Hill, R.J., Ruble, T.E., Pollastro, R.M., 2007. Unconventional shale-gas systems: the Mississippian Barnett Shale of north-central Texas as one model for thermogenic shale-gas assessment. Am. Assoc. Pet. Geol. Bull. 91, 523–533.

Martini, A.M., Walter, L.M., Budai, J.M., Ku, T.C.W., Kaiser, C.J., Schoell, M., 1998. Genetic and temporal relations between formation waters and biogenic methane—Upper Devonian Antrim Shale, Michigan basin, USA. Geochim. Cosmochim. Acta 62, 1699–1720.

Rooney, M.A., Claypool, G.E., Chung, H.M., 1995. Modeling thermogenic gas generation using carbon isotope ratios of natural gas hydrocarbons. Chem. Geol. 126, 219–232.

Schoell, M., 1983. Genetic characterization of natural gases. Am. Assoc. Pet. Geol. Bull. 67, 2225–2238.

Stahl, W.J., 1974. Carbon isotope fractionations in natural gases. Nature 251, 134–135.

Sweeney, J.J., Burnham, A.K., 1990. Evaluation of a simple model of vitrinite reflectance based on chemical-kinetics. Am. Assoc. Pet. Geol. Bull. 74, 1559–1570.

Tannenbaum, E., Kaplan, I.R., 1985. Role of minerals in the thermal alteration of organic matter—1: generation of gases and condensates under dry condition. Geochim. Cosmochim. Acta 49, 2589–2604.

Waples, D.W., 2000. The kinetics of in-reservoir oil destruction and gas formation: constraints from experimental and empirical data and from thermodynamics. Org. Geochem. 31, 553–575.

Welte, D.H., Schaefer, R.G., Yalçin, M.N., 1988. Gas generation from source rocks: aspects of a quantitative treatment. In: Schoell, M. (Ed.), Origins of Methane in the Earth. Chem. Geol. 71; 1988, pp. 105–116 (special issue).

Xiong, Y.Q., Geng, A.S., Liu, J.Z., 2004. Kinetic-simulating experiment combined with GC–IRMS analysis: application to identification and assessment of coal-derived methane from Zhongba Gas Field (Sichuan Basin, China). Chem. Geol. 213, 325–338.

Zhang, S.C., Zhang, B.M., Bian, L.Z., Jin, Z.J., Wang, D.R., Chen, J.F., 2007. The Xiamaling oil shale generated through Rhodophyta over 800 Ma ago. Sci. China Ser. D: Earth Sci. 50, 527–535.

Zou, C.N., Yang, Z., Dai, J.X., Dong, D.Z., Zhang, B.M., Wang, Y.M., Deng, S.H., Huang, J. L., Liu, K.Y., Yang, C., Wei, G.Y., 2015. The characteristics and significance of conventional and unconventional Sinian–Silurian gas systems in the Sichuan Basin, central China. Mar. Pet. Geol. 64, 386–402.

Zumberge, J., Ferworn, K., Brown, S., 2012. Isotopic reversal ('rollover') in shale gases produced from the Mississippian Barnett and Fayetteville formations. Mar. Pet. Geol. 31, 43–52.